CSIRO PUBLISHING

Aust. J. Chem.
http://dx.doi.org/10.1071/CH16224

Full Paper

Open-Chain Crown-Ether-Derived Two-Photon Fluorescence Probe for Real-Time Dynamic Biopsy of Mercury Ions

Chibao Huang,[A,E] *Daohai Zhang,*[B] *Junle Qu,*[C] *Xiaonan Liu,*[D,E] *Guanglian Zhao,*[A] *Tingxiang Yuan,*[A] *and Yang Liu*[A]

[A]Chemistry and Chemical Engineering College, Zunyi Normal University, Zunyi 563002, China.
[B]Research and Development Department (R & D), National Engineering Research Center for Compounding and Modification of Polymeric Materials, Guiyang 55004, China.
[C]Key Laboratory of Optoelectronic Devices and Systems of Ministry of Education and Guangdong Province, Shenzhen University, Shenzhen 518060, China.
[D]The Hospital Infection Management Section, The Affiliated Baiyun Hospital of Guizhou Medical University, Guiyang 550014, China.
[E]Corresponding authors. Email: huangchibao@163.com; liuxiaonan309@163.com

A novel two-photon fluorescence probe for Hg^{2+} derived from bis(styryl)terephthalonitrile, as a two-photon fluorophore, and bis[2-(2-hydroxyethyl sulfanyl) ethyl]amino group (ionophore), as a novel Hg^{2+} ligand, was developed. The probe possesses small molecule size, large two-photon absorption cross-section (1067 GM) in H_2O, non-cytotoxic effect, long wavelength emission at 588 nm, large Stokes shift (121 nm), excellent photostability, high water solubility, good cell permeability, and pH insensitivity in the biologically relevant range. The probe can selectively detect Hg^{2+} ions in live cells and living tissues without interference from other metal ions and the membrane-bound probes, and its quenching constant is $8.73 \times 10^5\ M^{-1}$.

Manuscript received: 23 August 2016.
Manuscript accepted: 17 October 2016.
Published online: 14 November 2016.

Introduction

Insights into the selective staining and/or imaging of specific cellular ions are of paramount importance for a deeper understanding of the character of each ion in a cellular system and their complex biological functions and processes.[1–3] Two-photon (TP) excitation fluorescence microscopy (TPM), which uses two photons of lower energy as the excitation source, has rapidly evolved into a widely used tool in biological and biomedical research.

Ion-targeting two-photon-excited fluorescence (TPEF) probes have increasingly drawn attention because of the laser light excitation capability of these probes. Such a capability offers several advantages including the possibility of performing deep tissue imaging, minimal photodamage to biological samples and bleaching to the probes, and low interference from the auto-fluorescence of the cell.[4–6] Various TPEF probes have been successfully designed and synthesised for the detection of lead ions,[7] zinc ions,[8–10] silver ions,[11,12] glucose,[13] cysteine or homocysteine,[14] thiols,[15] amyloid-β plaques,[16] and other small molecules[17] in the past few years.

Mercury and its derivatives are widely used in industry, which causes adverse environment and health problems.[18,19] Concerns over toxic exposure to mercury provide motivation to explore new methods for monitoring aqueous Hg^{2+} in living cells. Sensing of Hg^{2+} in plants and animals has been conducted by means of atomic absorption spectroscopy,[20] X-ray microanalysis,[21] and $^{203}Hg^{2+}$ detection. These techniques usually require expensive apparatus and/or sample preparation. Furthermore, they typically cause damage to the living organisms during analysis.[22] In contrast, fluorescent chemodosimeters provide a promising way for simple and rapid tracking of Hg^{2+} in biological systems. However, only a few of these fluorescent probes have been used successfully in living cells,[23] as fluorescent chemodosimeters for Hg^{2+} detection are often limited by nonspecific interference from Cu^{2+} and other competing metal ions[24,25] or are incompatible with aqueous media and living cells,[26] and/or delay Hg^{2+} response.[27]

Although many one-photon sensors for mercury ion have been developed,[28–31] only a few two-photon fluorescence chemodosimeters for mercury ion sensing have been reported.[32–34] Thus, it can be seen that the development of two-photon fluorescence sensors for mercury ion is not only indispensable to biological chemistry, but also really challenging.

Recently, we reported a TPEF probe for Hg^{2+} derived from 4-methyl-2,5-dicyano-4′-amino stilbene (**DCS**) as a TP fluorophore and bis[2-(2-hydroxyethyl sulfanyl)ethyl]amino group

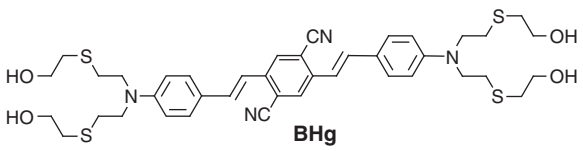

Fig. 1. Molecular structure of probe **BHg**.

(**HSA**) as a novel Hg^{2+} ligand.[12] Although this probe exhibited excellent selectivity for Hg^{2+}, it was not applied to live cell and living tissues imaging.

Herein, we extend our earlier work[12] and report a new TPEF probe for Hg^{2+} derived from bis(styryl)terephthalonitrile as a two-photon fluorophore and bis[2-(2-hydroxyethyl sulfanyl) ethyl]amino group (ionophore) as a novel Hg^{2+} ligand. The probe, 2,5-bis((*E*)-4-(bis(2-(2-hydroxyethylthio)ethyl)amino) styryl)terephthalonitrile (**BHg**), contains two sulfur atoms known as 'soft base' capable of chelating so-called 'soft acid' heavy metal cations and exhibits good affinity for Hg^{2+}. We report that **BHg** (Fig. 1) is capable of imaging Hg^{2+} ions in live cells without mistargeting and photobleaching problems.

Experimental

Materials and Methods

NMR spectra were recorded on a VARIAN INOVA 400 MHz NMR spectrometer. Mass spectral determinations were made on a electrospray ionisation quadrupole time-of-flight mass spectrometer (Micromass, UK). High-resolution mass spectrometry (HRMS) was performed on a gas chromatography time-of-flight mass spectrometer (Micromass, UK). Fluorescence measurements were performed on a PTI-C-700 Felix and Time-Master system. Fluorescence quantum yields (Φ) were measured using standard methods[35] on air-equilibrated samples at room temperature. Quinine bisulfate in 0.05 M H_2SO_4 ($\Phi = 0.546$) was used as a reference.[35] TPEF action cross-section spectra were recorded according to the experimental protocol established by Xu and Webb[36] using a mode-locked Ti/sapphire laser that delivers ~80 fs pulses at 76 MHz. Fluorescein (10^{-4} M in 0.1 M NaOH), whose TPEF action cross-sections are well known,[36] served as the reference. The quadratic dependence of the fluorescence intensity on the excitation intensity was verified for each data point, indicating that the measurements were carried out in intensity regimes in which saturation or photodegradation does not occur. The measurements were performed at room temperature on air-equilibrated solutions (10^{-5} M). The experimental uncertainty on the absolute action cross-sections determined by this method has been estimated to be ± 20 %.[36] Absorption spectra were measured on a HP-8453 spectrophotometer. Solvents were generally dried and distilled before use. Reactions were monitored by thin layer chromatography on Merck silica gel 60 F_{254} pre-coated aluminium sheets. Column chromatography was performed using Merck silica gel Si 60 (40–63 μm, 230–400 mesh). The pH-dependent fluorescence studies were performed according to the literature.[37]

Synthesis

*2,5-Bis((E)-4-(bis(2-chloroethyl)amino)styryl) terephthalonitrile (**8**)*

Aldehyde **2** (560 mg, 2.28 mmol) and NaH (55 mg, 2.28 mmol) were dissolved in tetrahydrofuran (THF; 3 mL), and the solution was cooled to 0°C under N_2. To this solution, phosphonate **7** (488 mg,1.14 mmol) in THF (9 mL) was added dropwise. The reaction mixture was stirred for 1 h at 0°C, and then for 12 h at room temperature, followed by the removal of THF under reduced pressure. Water was added to the reaction mixture, and the product was extracted with dichloromethane (4 × 10 mL). The organic layer was dried with dry Na_2SO_4, followed by evaporation of the solvent. The crude product was separated by column chromatography with a gradient of hexane in dichloromethane (20–0 %) and ethyl acetate in dichloromethane (0–20 %). The resulting solid was recrystallised from acetone to give compound **8** (453 mg, 65 %) as a yellow powder.

ν_{max} (KBr)/cm^{-1} 2223 (C≡N) and 1594–1348 (C=C). δ_H ([D6]DMSO, 400 MHz) 8.446 (2H, s, Ph), 7.620 (2H, d, *J* 16.4, *CH*=CH), 7.498 (4H, d, *J* 8.4, Ph), 7.054 (2H, d, *J* 16.4, *CH*=CH), 6.844 (4H, d, *J* 8.8, Ph), 3.772 (8H, t, $J_1 = J_2$ 4.4 Hz, N*CH*$_2$), 3.712 (8H, t, $J_1 = J_2$ 2 Hz, *CH*$_2$Cl). Found: C 62.80, H, 4.98, Cl 23.13, N 9.10 %; $[M]^+$ 610.1225. Anal. Calc. for $C_{32}H_{30}Cl_4N_4$ (612.42) C 62.76, H 4.94, Cl 23.16, N 9.15 %; $[M]^+$ 610.1225.

*2,5-Bis((E)-4-(bis(2-(2-hydroxyethylthio)ethyl)amino) styryl)terephthalonitrile (**BHg**)*

Compound **8** (306 mg, 0.5 mmol), 2-mercaptoethanol (172 mg, 2.2 mmol), and anhydrous K_2CO_3 (414 mg, 3 mmol) were dissolved in acetone (25 mL). Then, the mixture was refluxed for 24 h with stirring under N_2. The resulting mixture was filtered, and the filtrate was concentrated by evaporating the solvent to obtain a viscous liquid. The crude product was purified by column chromatography using acetone/dichloromethane to afford compound **BHg** (335 mg, 86 %) as a red solid. Further purification could be achieved by recrystallisation from methanol to give needles.

ν_{max} (KBr)/cm^{-1} 3422 (OH), 2922 (CH), 2220 (C≡N), 1631–1349 (C=C). δ_H ([D]$CHCl_3$, 400 MHz) 8.442 (2H, s, Ph), 7.620 (2H, d, *J* 16.0, CH=*CH*), 7.513 (4H, d, *J* 8.8, Ph), 7.055 (2H, d, *J* 16.0, CH=*CH*), 6.789 (4H, d, *J* 8.4, Ph), 4.918 (8H, t, *J* 4.8, 4 × O*CH*$_2$), 3.633 (8H, t, $J_1 = J_2$ 6.0, 4 × N*CH*$_2$), 2.791 (8H, t, J_1 6.8, J_2 7.6, 4 × S*CH*$_2$), 2.728 (8H, t, J_1 6.8, J_2 6.4, 4 × S*CH*$_2$), 2.564 (4H, s, 4 × O*H*). δ_C ([D]$CHCl_3$, 100 MHz) 147.68, 138.02, 134.96, 129.36, 128.88, 123.48, 117.03, 116.12, 113.15, 111.64, 61.23, 50.69, 34.11, 28.69. Found: C 61.71, H 6.54, N 7.16, O 8.17, S 16.42 %; $[M]^+$ 778.2715. Anal. Calc. for $C_{40}H_{50}N_4O_4S_4$ (778.2715) C 61.66, H 6.47, N 7.19, O 8.21, S 16.46 %; $[M]^+$ 778.2715.

Results and Discussion

*Design and Synthesis of **BHg***

2,5-Dibromo-*p*-xylene (**4**),[38] 2,5-dimethyl-terephthalonitrile (**5**),[38] 2,5-bis(bromomethyl)terephthalonitrile (**6**),[38] 1,4-bis (diethylphosphorylmethyl)-2,5-dicyano-benzene (**7**),[39] and 4-[bis(2-chloro-ethyl)amino]benzaldehyde (**2**)[40] were synthesised according to literature procedures. The nucleophilic substitution of **8** and 2-mercaptoethanol gave **BHg** in high yield (86 %) (Scheme 1). In the reaction of **8** and 2-mercaptoethanol, the substitution of the mercapto group, rather than the hydroxy group, for chloro group was observed because the nucleophilic strength of the mercapto group is superior to that of the hydroxy group.

*Selectivity of Sensor **BHg** for Metal Ions*

The solubility of **BHg** in water was 576 μM, which is sufficient to stain the cells (Fig. S1, available as Supplementary Material). To obtain insights into the binding properties of **BHg** towards

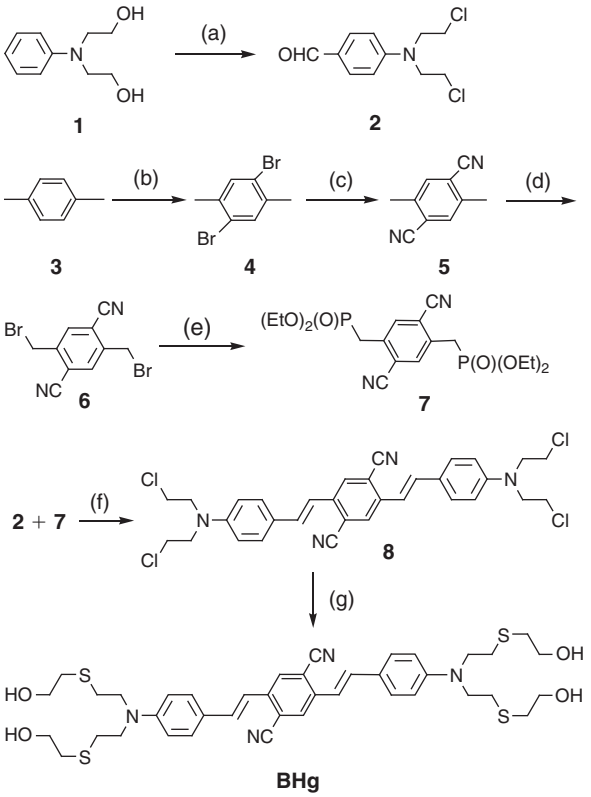

Scheme 1. Synthetic procedures of compound **BHg** (reagent and conditions: (a) $POCl_3$/DMF, 90°C, 2 h (95 % yield); (b) Br_2/CH_2Cl_2, no light, 20°C, 24 h (90 % yield); (c) CuCN/DMF, 150°C, 48 h (78 % yield); (d) *N*-bromosuccinimide (NBS)/CCl_4, 6 h (15 % yield); (e) $P(OEt)_3$/toluene, 120°C, 5 h (96 % yield); (f) NaH (2 equiv.)/THF, 12 h (65 % yield); (g) K_2CO_3/MeCN, $HS(CH_2)_2OH$, 40°C, 12 h (86 % yield).

metal ions, the fluorescence spectral changes were investigated upon addition of various metal ions (Ag^+, Ca^{2+}, Cd^{2+}, Cr^{3+}, Fe^{3+}, Co^{2+}, Ni^{2+}, Fe^{2+}, Na^+, Cu^{2+}, Zn^{2+}, Mn^{2+}, Mg^{2+}, Hg^{2+}, Pb^{2+}, K^+, and Ba^{2+}) to 30 mM MOPS buffer (100 mM KCl, 10 mM EGTA, pH 7.2; EGTA = ethylene glycol-bis(2-aminoethylether)-*N*,*N*,*N*′,*N*′-tetraacetic acid and MOPS = 3-(morpholino)propanesulfonic acid) of **BHg** (Fig. 2). The experimental results suggest that **BHg** shows a notable selectivity towards Hg^{2+}. As depicted in Fig. 2, **BHg** displays scarcely any response to other metal ions and weak complexation with Ag^+, Pb^{2+}, and Cu^{2+}. The highly selective recognition of **BHg** for mercury ion can be attributed to two factors. On the one hand, a sulfur atom and Hg^{2+} are typical 'soft base' and 'soft acid', respectively, and the very strong affinity between them is quite natural. On the other hand, the nitrogen atom properties and the numbers of sulfur atoms in open-chain monoazadithiacrown ether may play an important role on the affinities displayed by nitrogen and sulfur atoms towards heavy metal ions.

*Sensitivity of Sensor **BHg** towards Hg^{2+} in UV-Visible, and One- and Two-Photon-Excited Fluorescence Spectra*

Notably, upon complexation with Hg^{2+}, two characteristic strong absorption bands of **BHg** shifted from 467 and 269 nm to 426 and 284 nm, respectively – a hypochromatic shift of 41 nm and a bathochromic shift of 15 nm occurred with the cation-binding event. Additionally, the intensity of the absorption bands centred at 467 nm and 269 nm declined and enhanced

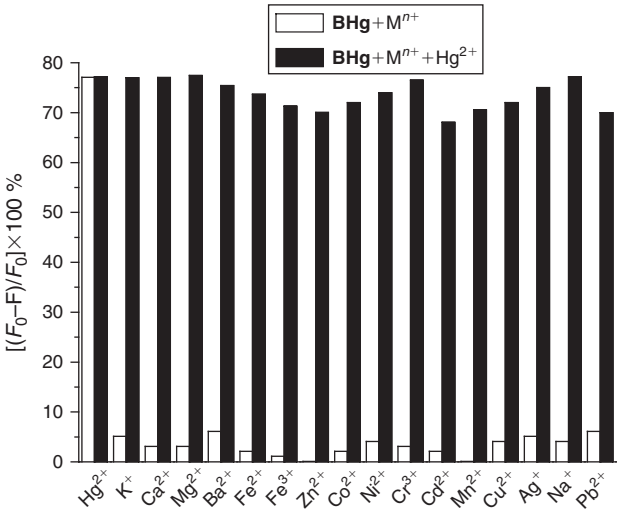

Fig. 2. Comparison of the percentage quenching of one-photon-excited fluorescence of **BHg** (1 μM) at 588 nm in the presence of 20 mM Zn^{2+}, K^+, Ca^{2+}, Mg^{2+}, Ba^{2+}, Fe^{2+}, Fe^{3+}, Pb^{2+}, Co^{2+}, Ni^{2+}, Cr^{3+}, Cd^{2+}, Mn^{2+}, Cu^{2+}, Ag^+, Na^+, or Pb^{2+} (non-filled bars), followed by addition of 40 μM Hg^{2+} (filled bars). These data were measured in 30 mM MOPS buffer (100 mM KCl, 10 mM EGTA, pH 7.2).

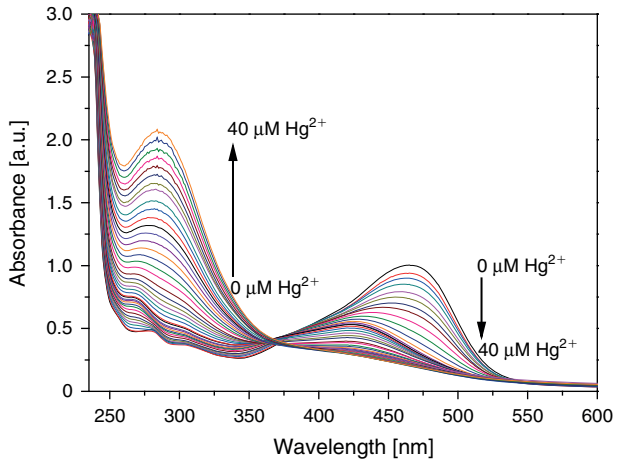

Fig. 3. Absorption spectra of **BHg** (10 μM) in 30 mM MOPS buffer (100 mM KCl, 10 mM EGTA, pH 7.2) in the presence of free Hg^{2+} (0–40 μM).

gradually, respectively, upon addition of Hg^{2+} at increasing concentrations (Fig. 3). The quenching constants (K_{sv}^{Ab}; sv = Stern Volmer; Ab = absorption) of **BHg** for mercury ion were determined from the absorption-titration curves to be 8.24×10^5 M^{-1} (one stage quenching constant) and 4.36×10^4 M^{-1} (two stage quenching constant) at 20°C in 30 mM MOPS buffer (Fig. S2, Supplementary Material).

BHg exhibits a very strong sensitivity towards Hg^{2+} in the one-photon (OP) and TP processes (Figs 4 and 5), and the emission band of **BHg** centred at 587 nm progressively decreased upon addition of Hg^{2+} to the solution. The quenching of **BHg** shows a downward, non-linear curvature in the Stern–Volmer plot (I_{587} versus [Hg^{2+}], where I_{587} refers to the luminescence intensity measured at 587 nm) in a broader Hg^{2+} concentration range (0–40 μM) (Figs S3 and S5, Supplementary Material). The quenching constants (K_{sv}^{OP} and K_{sv}^{TP}) for

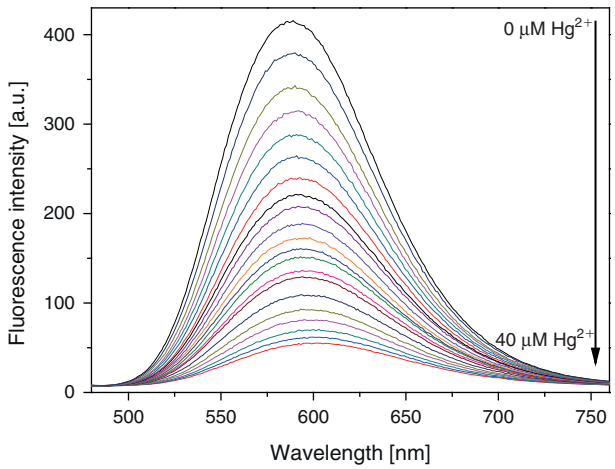

Fig. 4. OP emission spectra of **BHg** (1.0 μM) in 30 mM MOPS buffer (100 mM KCl, 10 mM EGTA, pH 7.2) in the presence of free Hg^{2+} (0–40 μM).

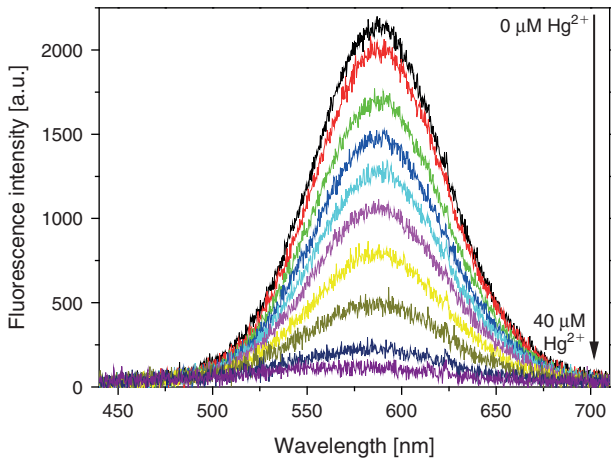

Fig. 5. TP emission spectra of **BHg** (1.0 μM) in 30 mM MOPS buffer (100 mM KCl, 10 mM EGTA, pH 7.2) in the presence of free Hg^{2+} (0–40 μM).

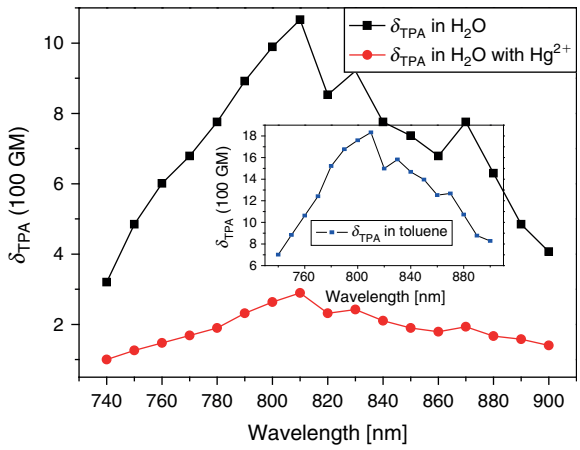

Fig. 6. Two-photon excitation spectra of **BHg** (1.0 μM) before (■) addition of 20 equiv. Hg^{2+} in toluene, and before (■) and after (●) addition of 20 equiv. Hg^{2+} in 30 mM MOPS buffer (100 mM KCl, 10 mM EGTA, pH 7.2). TPA, Two-photon absorption.

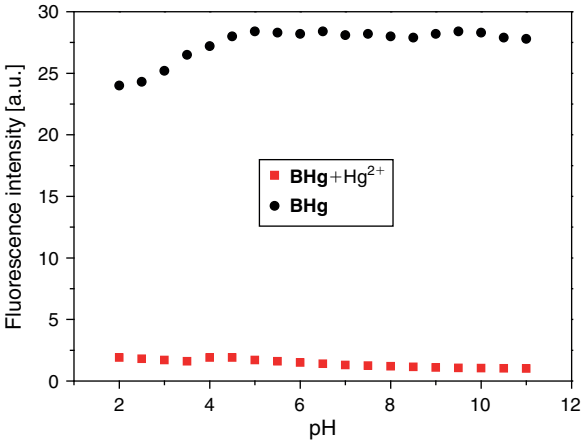

Fig. 7. Effect of pH on the one-photon fluorescence intensity of 1.0 μM **BHg** in the presence of 0.0 μM (●) and 1.0 μM (■) free Hg^{2+}. The solution pH was adjusted with HCl, NaCl, and/or NaOH. The excitation wavelength was 467 nm.

BHg calculated from the OP and TP fluorescence titration curves (Figs 4 and 5) are 5.25×10^5 M^{-1} (2.76×10^4 M^{-1}) and 6.94×10^5 M^{-1} (2.24×10^4 M^{-1}) (Figs S3 and S5), respectively; the detection limit of the probe is in the micromolar range. However, in a narrower concentration range (0.10–10 μM), two linear Stern–Volmer plots are obtained with Stern–Volmer constants of $K_{sv}^{OP} = 8.59 \times 10^5$ M^{-1} and $K_{sv}^{TP} = 8.73 \times 10^5$ M^{-1} (Figs S4 and S6, Supplementary Material). **BHg** is strongly fluorescent in CH_2Cl_2 ($\Phi = 0.83$) and H_2O ($\Phi = 0.62$). This means that **BHg** can serve as a good sensor for mercury ion applied to one-photon fluorescence (OPF) and two-photon fluorescence (TPF) detection.

*Job's Plot for **BHg**–Hg^{2+} Complex*

For determining the complexation ratio between the ligand and the metal ion, a Job plot experiment was conducted by varying the concentration of both **BHg** and Hg^{2+}. Solutions of **BHg** and Hg^{2+} in 30 mM MOPS buffer in different mole fractions were prepared by mixing **BHg** and Hg^{2+} in H_2O in appropriate ratios while maintaining the total concentration to 1.0 μM. The absorbance of each solution at 467 nm was measured. The concentration of **BHg**–Hg^{2+} complex for each solution was calculated by using the UV absorption data and the quenching constant (Fig. S4). The plot of [complex] versus the mole fraction of Hg^{2+} shows a maximum when the mole fraction is 0.67, indicating that **BHg** is coordinated with Hg^{2+} with 1 : 2 stoichiometry in water solution. (Fig. S7).

*Two-Photon Absorption Cross-Section of **BHg** versus Two-Photon-Excited Wavelength*

The two-photon absorption cross-section (δ) of **BHg** was determined by using the two-photon-induced fluorescence measurement technique.[36] As expected, δ of **BHg** decreased 2.7-fold from 1067 to 294 GM upon addition of 20 μM Hg^{2+} to the solution (Fig. 6). TP excitation of **BHg** produced similar emission spectra to those generated by OP excitation. Likewise, its two-photon excitation spectra is analogous to the OP absorption spectra, and it had a TP excitation maximum at 810 nm. When excess Hg^{2+} was added, δ decreased further, probably because the electron-donating ability of the aromatic amino moiety is attenuated upon complexation.

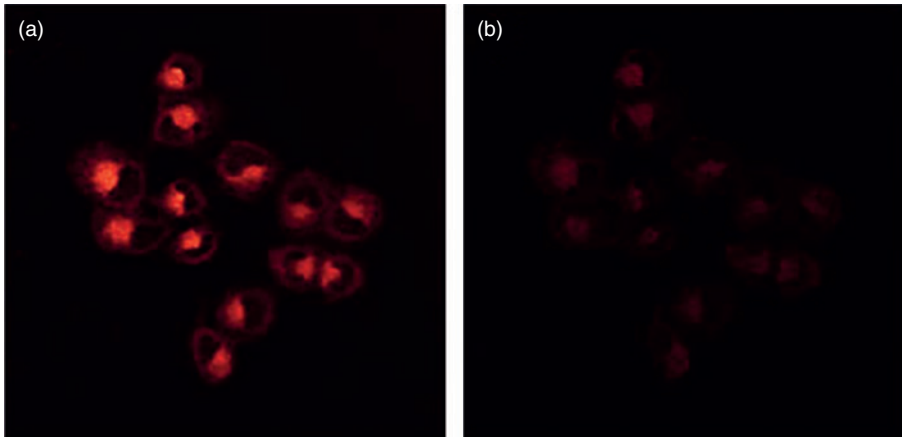

Fig. 8. TPM images of 1.0 μM **BHg**-labelled mouse fibroblast collected at 550–650 nm (a) before and (b) after addition of 20 μM Hg^{2+} to the imaging solution. The TPEF images were collected upon excitation at 810 nm with a femtosecond pulse. Images shown are representative images obtained from replicate experiments ($n = 5$).

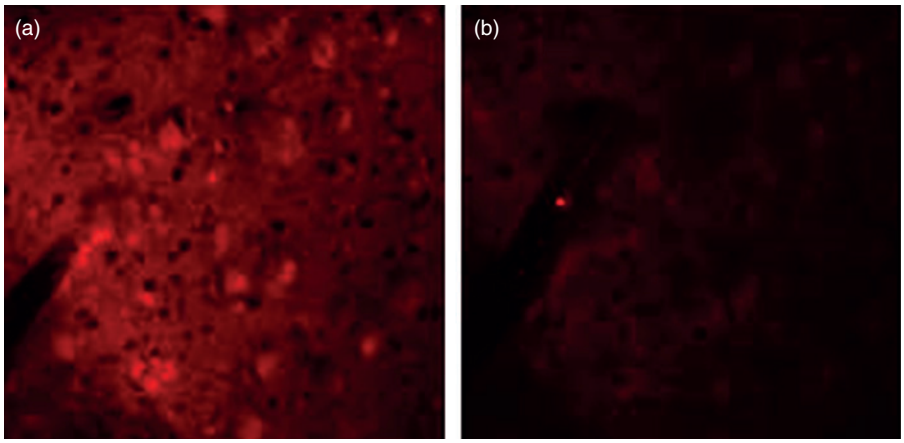

Fig. 9. TPM images of a mouse brain tissue slice stained with 10.0 μM **BHg** at a depth of ~120 μm at a magnification of 100 × (a) before and (b) after addition of 20.0 μM Hg^{2+} to the imaging solution. The TPEF images were collected at 550–650 nm upon excitation at 810 nm with a femtosecond pulse. Images shown are representative images obtained from replicate experiments ($n = 5$).

*One-Photon Fluorescence Spectra of Sensor **BHg** versus pH*

The fluorescence of **BHg** was also slightly weakened by protonation of the tertiary amine in the bis(styryl)terephthalonitrile skeleton at pH < 4.5 or so, and remained unchanged at pH 4.5–13 (Fig. 7). The enhancement of the fluorescence at high pH and quenching by H^+ and Hg^{2+} are consistent with an intramolecular charge transfer mechanism from the aromatic amines. Therefore, **BHg** is pH-insensitive in the biologically relevant pH range.

Two-Photon Scanning Microscopy Imaging

For two-photon in vitro imaging, cells were imaged in the tissue culture chamber (5 % CO_2, 37°C) using a Zeiss 510 LSM (upright configuration) confocal microscope equipped with a femtosecond-pulsed Ti:sapphire laser (Mira 900-F, Coherent). The excitation beam produced by the femtosecond laser, which was tuneable from 700 to 1100 nm ($\lambda_{ex} = 810$ nm, ~1.5 W), passed through an LSM 510 microscope equipped with an HFT 650 dichroic filter (Carl Zeiss, Inc.) and focussed onto the coverslip-adherent cells using a 63× oil immersion objective (numerical aperture of 1.4). The NLO META scan head allowed data collection in 10.7-nm windows at 610 nm, and a bypass filter of 550–650 nm was used for collection of the emission light.

Details of the preparation of the mouse fibroblast culture are given in the Supplementary Material. The TPM images of mouse fibroblast labelled with **BHg** showed very strong TPF at 550–650 nm (Fig. 8a), and high contrast and good resolution were observed, indicating **BHg** has a considerably desirable cell-imaging effect and good cell permeability. After addition of 20 μM Hg^{2+} to the imaging solution and incubation at 37°C under 5 % CO_2 for 15 min, the TPF intensity decreased rapidly, and the TPM image became shaded and obscure (Fig. 8b). Without interference from the membrane-bound probes (as indicated from the lack of fluorescence at 360–460 nm) in this visual window, **BHg** can detect Hg^{2+} in live cells and displays no cytotoxic effects.

To further investigate the utility of this probe in deep tissue imaging, TPM images were obtained from a part of a mouse brain tissue slice incubated with 10.0 μM **BHg** for 30 min at 37°C. Two TPM images were obtained in the same plane at a depth of ~120 μm. In the absence of Hg^{2+} addition, the TPM image was bright (Fig. 9a), whereas upon addition of Hg^{2+}, the

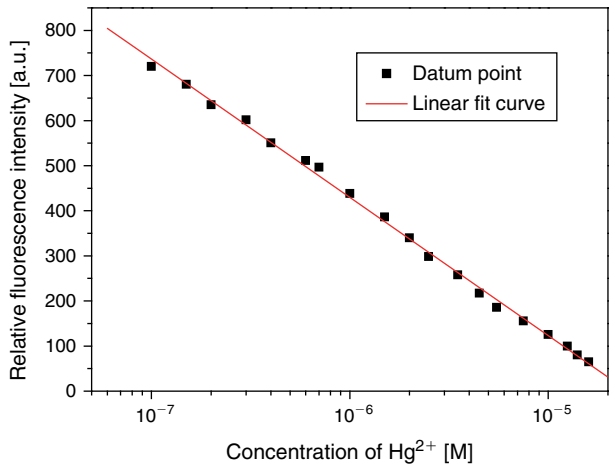

Fig. 10. Calibration curve of the TPF intensities for **BHg** (1.0 μM) measured at 587 nm as a function of Hg^{2+} concentration ranging from 1.0×10^{-7} to 1.6×10^{-5} M.

emission was clearly diminished (Fig. 9b). This result demonstrates that **BHg** is capable of detecting intracellular Hg^{2+} ions at a depth of 120 μm in living tissues by using TPM.

*Building a Calibration Curve for a Hg^{2+}–**BHg** Complex*

All reagents were of the highest purity available and at least of analytical reagent grade. The standard stock solution of lead(II) is prepared by dissolving the appropriate amount of mercury nitrate and a small amount of HNO_3 in double-distilled water. A series of standard solutions of Hg^{2+} at different concentrations are prepared by appropriate dilution of the stock solution with water and calibrated by volumetric analysis. As seen in Fig. S6, the TPF intensities of **BHg** (1.0 μM) show a linear correlation with Hg^{2+} concentrations from 1.0×10^{-7} to 1.6×10^{-5} M. The TPF intensities are plotted versus the solution standard concentrations, and the points should form a straight line. This line, called a calibration curve, shows how the TPF intensity changes as a function of the concentration of a solution.

A calibration curve of the TPF intensities for **BHg** (1.0 μM) versus the Hg^{2+} concentration varied from 1.0×10^{-7} to 1.6×10^{-5} M was obtained by fitting a linear equation to the data in Table S1 in Supplementary Material. The calibration curve can be described by Eqn 1 (Fig. 10). As deduced from Fig. 10, the correlation coefficient (r) and the population correlation coefficient (ρ) are 0.99888 and <0.0001, respectively. This result indicates that there is a good linear correlation between the TPF intensities and the Hg^{2+} concentration ranging from 1.0×10^{-7} to 1.6×10^{-5} M.

$$Y = -2407.07 - 13536.52\log[Hg^{2+}] \quad (1)$$

Conclusion

In conclusion, we have developed a TPF probe **BHg** with small molecule size, large TP absorption cross-section (1067 GM), non-cytotoxic effect, long wavelength emission at 587 nm (adjacent to the ideal imaging visual window 650–900 nm), large Stokes shift (120 nm), excellent photostability, moderate water solubility, and good cell permeability. **BHg** is pH-insensitive in the biologically relevant range, and its quenching constant (K_{sv}^{TP}) is 8.73×10^5 M^{-1}. This novel probe can selectively detect Hg^{2+} ions in live cells and living tissues at a depth of 120 μm without interference from other metal ions and the membrane-bound probes.

Supplementary Material

Photophysical study, cell culture, two-photon imaging, and NMR spectra are available on the Journal's website.

Acknowledgements

Financial supports from the National Natural Science Foundation of China (Grant No. 21562050), Special Fund Project of the construction of the Eighth Batch of Scientific and Technological Innovation Talent Team in Guizhou Province (Grant No. (2015)4007), Guizhou Science and Technology Fund Project (Grant Nos J[2015]2146, J LKZS [2012]23, J LKZS [2012]13), Key Project of Education Department of Guizhou Province (Grant Nos KY [2014]296, KY(2013)171), Teaching Contents and Curriculum System Reform Project of Higher Education in Guizhou Province (Grant No. KY [2014] JXGChcb), Project of '15851 Talents Elite Project' in Zunyi City (Grant No. (2015)4007), and the Science and Technology Project of Zunyi city Honghuagang District (Grant No. [2015]18) are deeply acknowledged.

References

[1] H. M. Kim, C. Jung, B. R. Kim, S.-Y. Jung, J. H. Hong, Y.-G. Ko, K. J. Lee, B. R. Cho, *Angew. Chem., Int. Ed.* **2007**, *46*, 3460. doi:10.1002/ANIE.200700169

[2] H. M. Kim, B. R. Kim, J. H. Hong, J.-S. Park, K. J. Lee, B. R. Cho, *Angew. Chem., Int. Ed.* **2007**, *46*, 7445. doi:10.1002/ANIE.200701720

[3] M. K. Kim, C. S. Lim, J. T. Hong, J. H. Han, H.-Y. Jang, H. M. Kim, B. R. Cho, *Angew. Chem., Int. Ed.* **2010**, *49*, 364. doi:10.1002/ANIE.200904835

[4] B. R. Masters, *Confocal Microscopy and Multiphoton Excitation Microscopy: The Genesis of Live Cell Imaging* **2006** (SPIE: Bellingham, WA).

[5] P. T. C. So, C. Y. Dong, B. R. Masters, K. M. Berland, *Annu. Rev. Biomed. Eng.* **2000**, *2*, 399. doi:10.1146/ANNUREV.BIOENG.2.1.399

[6] L. Guo, M. S. Wong, *Adv. Mater.* **2014**, *26*, 5400. doi:10.1002/ADMA.201400084

[7] C. Huang, C. Ding, *Anal. Chim. Acta* **2011**, *699*, 198. doi:10.1016/J.ACA.2011.05.015

[8] C. Huang, J. Qu, J. Qi, M. Yan, G. Xu, *Org. Lett.* **2011**, *13*, 1462. doi:10.1021/OL200146J

[9] S. Sumalekshmy, M. M. Henary, N. Siegel, P. V. Lawson, Y. Wu, K. Schmidt, J.-L. Brédas, J. W. Perry, C. J. Fahrni, *J. Am. Chem. Soc.* **2007**, *129*, 11888. doi:10.1021/JA073240O

[10] H. M. Kim, M. S. Seo, M. J. An, J. H. Hong, Y. S. Tian, J. H. Choi, O. Kwon, K. J. Lee, B. R. Cho, *Angew. Chem., Int. Ed.* **2008**, *47*, 5167. doi:10.1002/ANIE.200800929

[11] C. Huang, A. Ren, C. Feng, N. Yang, *Sens. Actuators, B* **2010**, *151*, 236. doi:10.1016/J.SNB.2010.09.013

[12] C. Huang, X. Peng, Z. Lin, J. Fan, A. Ren, D. Sun, *Sens. Actuators, B* **2008**, *133*, 113. doi:10.1016/J.SNB.2008.02.010

[13] Y. S. Tian, H. Y. Lee, C. S. Lim, J. Park, H. M. Kim, Y. N. Shin, E. S. Kim, H. J. Jeon, S. B. Park, B. R. Cho, *Angew. Chem., Int. Ed.* **2009**, *48*, 8027. doi:10.1002/ANIE.200901175

[14] M. Zhang, M. Yu, F. Li, M. Zhu, M. Li, Y. Gao, L. Li, Z. Liu, J. Zhang, D. Zhang, T. Yi, C. Huang, *J. Am. Chem. Soc.* **2007**, *129*, 10322. doi:10.1021/JA073140I

[15] J. H. Lee, C. S. Lim, Y. S. Tian, J. H. Han, B. R. Cho, *J. Am. Chem. Soc.* **2010**, *132*, 1216. doi:10.1021/JA9090676

[16] C. H. Heo, A. R. Sarkar, S. H. Baik, T. S. Jung, J. J. Kim, H. Kang, I. Mook-Jung, H. M. Kim, *Chem. Sci.* **2016**, *7*, 4600. doi:10.1039/C6SC00355A

[17] H. M. Kim, B. R. Cho, *Chem. Rev.* **2015**, *115*, 5014. doi:10.1021/CR5004425

[18] H. H. Harris, I. J. Pickering, G. N. George, *Science* **2003**, *301*, 1203. doi:10.1126/SCIENCE.1085941

[19] M. Harada, *Crit. Rev. Toxicol.* **1995**, *25*, 1. doi:10.3109/10408449509089885
[20] C. M. Palmeira, A. J. Moreno, V. M. Madeira, *Toxicol. Appl. Pharmacol.* **1994**, *127*, 50. doi:10.1006/TAAP.1994.1138
[21] T. Endo, M. Sakata, Z. A. Shaikh, *Toxicol. Appl. Pharmacol.* **1995**, *132*, 36. doi:10.1006/TAAP.1995.1084
[22] C. C. Bridges, R. K. Zalups, *Am. J. Pathol.* **2004**, *165*, 1385. doi:10.1016/S0002-9440(10)63396-2
[23] Z. Zhang, D. Wu, X. Guo, X. Qian, Z. Lu, Q. Xu, Y. Yang, L. Duan, Y. He, Z. Feng, *Chem. Res. Toxicol.* **2005**, *18*, 1814. doi:10.1021/TX0501536
[24] Z. Xu, X. Qian, J. Cui, *Org. Lett.* **2005**, *7*, 3029. doi:10.1021/OL051131D
[25] R. Martınez, A. Espinosa, A. T'arraga, P. Molina, *Org. Lett.* **2005**, *7*, 5869. doi:10.1021/OL052508I
[26] L. Prodi, C. Bargossi, M. Montalti, N. Zaccheroni, N. Su, J. S. Bradshaw, R. M. Izatt, P. B. Savage, *J. Am. Chem. Soc.* **2000**, *122*, 6769. doi:10.1021/JA0006292
[27] K. Rurack, M. Kollmannsberger, U. Resch-Genger, J. Daub, *J. Am. Chem. Soc.* **2000**, *122*, 968. doi:10.1021/JA992630A
[28] J. Greeley, W. P. Krekelberg, M. Mavrikakis, *Angew. Chem.* **2004**, *116*, 4396. doi:10.1002/ANGE.200454062
[29] H. Zheng, Z.-H. Qian, L. Xu, F.-F. Yuan, L.-D. Lan, J.-G. Xu, *Org. Lett.* **2006**, *8*, 859. doi:10.1021/OL0529086
[30] E. M. Nolan, S. J. Lippard, *J. Am. Chem. Soc.* **2003**, *125*, 14270. doi:10.1021/JA037995G
[31] H. Dai, F. Liu, Q. Gao, T. Fu, X. Kou, *Luminescence* **2011**, *26*, 523. doi:10.1002/BIO.1264
[32] Y. Wu, Y. Dong, J. Li, X. Huang, Y. Cheng, C. Zhu, *Chem. – Asian J.* **2011**, *6*, 2725. doi:10.1002/ASIA.201100534
[33] C. S. Lim, D. W. Kang, Y. S. Tian, J. H. Han, H. L. Hwang, B. R. Cho, *Chem. Commun.* **2010**, *46*, 2388. doi:10.1039/B922305C
[34] J. Bell, I. Samb, P. Y. Toullec, O. Mongin, M. Blanchard-Desce, V. Michelet, I. Leray, *New J. Chem.* **2014**, *38*, 1072. doi:10.1039/C3NJ01308A
[35] D. F. Eaton, *J. Photochem. Photobiol., B.* **1988**, *2*, 523. doi:10.1016/1011-1344(88)85081-4
[36] C. Xu, W. W. Webb, *J. Opt. Soc. Am. B* **1996**, *13*, 481. doi:10.1364/JOSAB.13.000481
[37] S. C. Burdette, G. K. Walkup, B. Spingler, R. Y. Tsien, S. J. Lippard, *J. Am. Chem. Soc.* **2001**, *123*, 7831. doi:10.1021/JA010059L
[38] H. Huang, Q. He, H. Lin, F. Bai, Z. Sun, Q. Li, *Polym. Adv. Technol.* **2004**, *15*, 84. doi:10.1002/PAT.453
[39] W. Wenseleers, F. Stellacci, T. Meyer-Friedrichsen, T. Mangel, C. A. Bauer, S. J. K. Pond, S. R. Marder, J. W. Perry, *J. Phys. Chem. B* **2002**, *106*, 6853. doi:10.1021/JP014675F
[40] R. H. Wiley, G. Irick, *J. Org. Chem.* **1961**, *26*, 593. doi:10.1021/JO01061A606